JET PROPULSION LABORATORY
CALIFORNIA INSTITUTE OF TECHNOLOGY

INTEROFFICE MEMORANDUM
IOM 335-JW,DB,WF-20080314-001
March 14, 2008

To: Lunar Distribution

From: J. G. Williams, D. H. Boggs and W. M. Folkner

Subject: DE421 Lunar Orbit, Physical Librations, and Surface Coordinates

Introduction

This memo discusses the DE421 lunar orbit, orientation angles and coordinate frames. The DE421 orbit is compared with DE403 and DE418. The construction of the lunar part of DE421 is described. For coordinate frames rotating with the Moon, two choices are described and the rotation between the two frames is given.

The planetary and lunar ephemeris DE421 (Folkner et al., 2008) was provided for the Phoenix mission to Mars. Also updated were the orbit and physical librations of the Moon. This memo concentrates on the lunar aspects of DE421.

DE421 vs. DE418 and DE403 Moon

DE403 was generated in 1995 and, compared to the recent DE418 and DE421 ephemerides, the lunar position is separating. DE418 is described by Folkner et al. (2007) and lunar aspects are discussed in Williams and Folkner (2007). The DE418–DE403 difference illustrated in Figure 1 shows the differences in radius as well as ecliptic longitude and latitude from 1990 to 2020. Figure 2 shows similar plots for DE421–DE403. The longitude difference shows the t^2 behavior from a 0.8% change in secular tidal acceleration, and the growing monthly variation in radius difference reflects the related acceleration of mean anomaly difference. A half meter separation in mean radius is due to a difference in the GM of Earth+Moon. The latitude pattern results from two monthly oscillations beating together while the amplitude of one increases due to the secular acceleration difference. The position difference is typically about 6 m in 2008, increasing to ~8 m in 2012, ~11 m in 2015, and ~16 m in 2020. The difference is mainly orthogonal to radius so corresponding angles are about 3, 4, 6, and 9 milliseconds of arc, respectively.

The lunar orbits of DE418 and DE421 are compared over 30 years in Figure 3 and are similar. The radial coordinates differ by a few centimeters and the two orthogonal components differ by a few decimeters. The ecliptic latitude and longitude differences are a few milliseconds of arc (mas). There is a slow drift of ~3 μas/yr in longitude differences and the 18.6 yr periodicity (node precession period) is due to small differences between diurnal and semidiurnal tides on Earth. Both DE418 and DE421 are superior to DE403 for navigation purposes. The accuracy of DE403 is degrading at an accelerating pace and it is no longer recommended for missions.

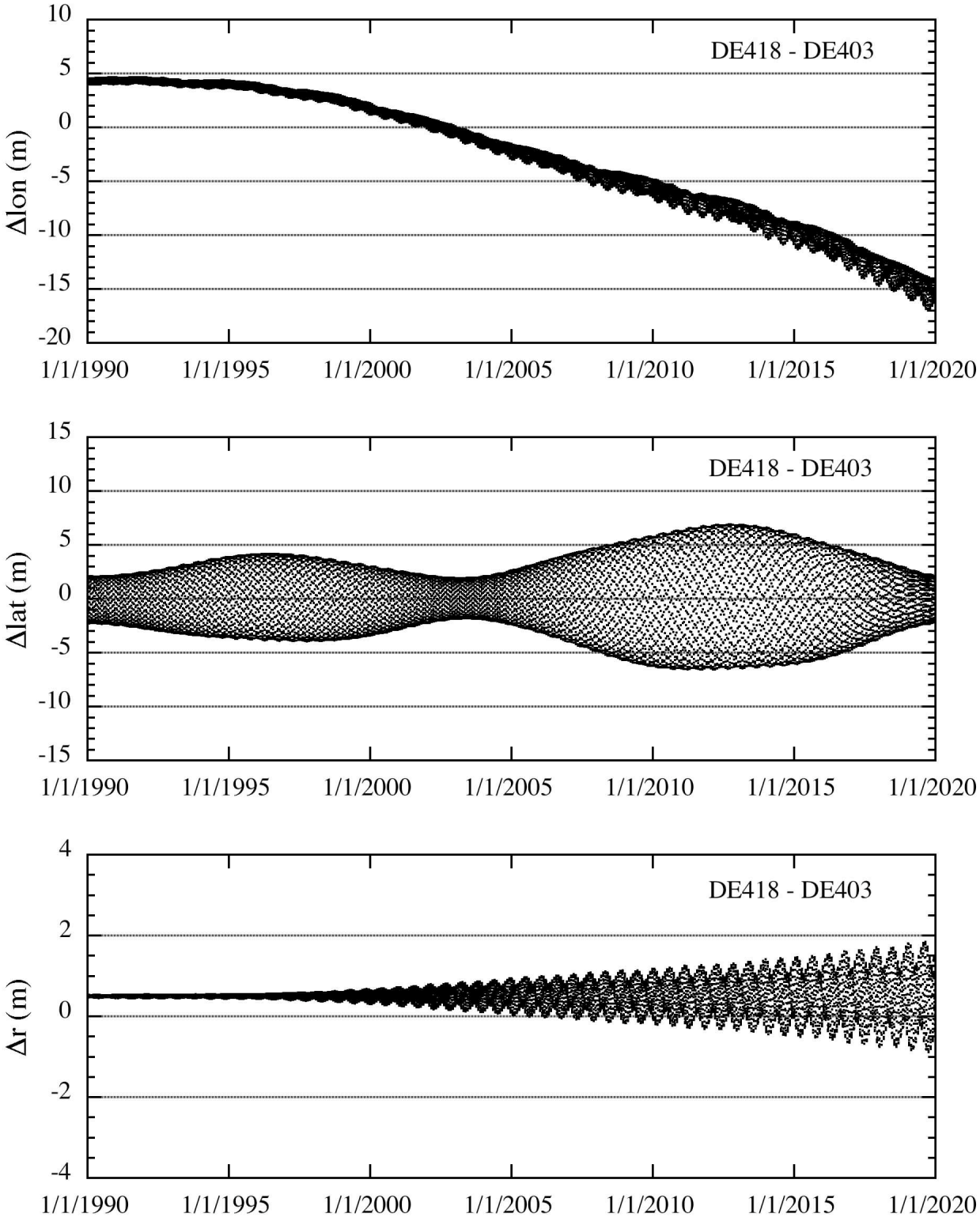

Figure 1. Moon differences for ecliptic longitude and latitude, and radius for DE418 – DE403.

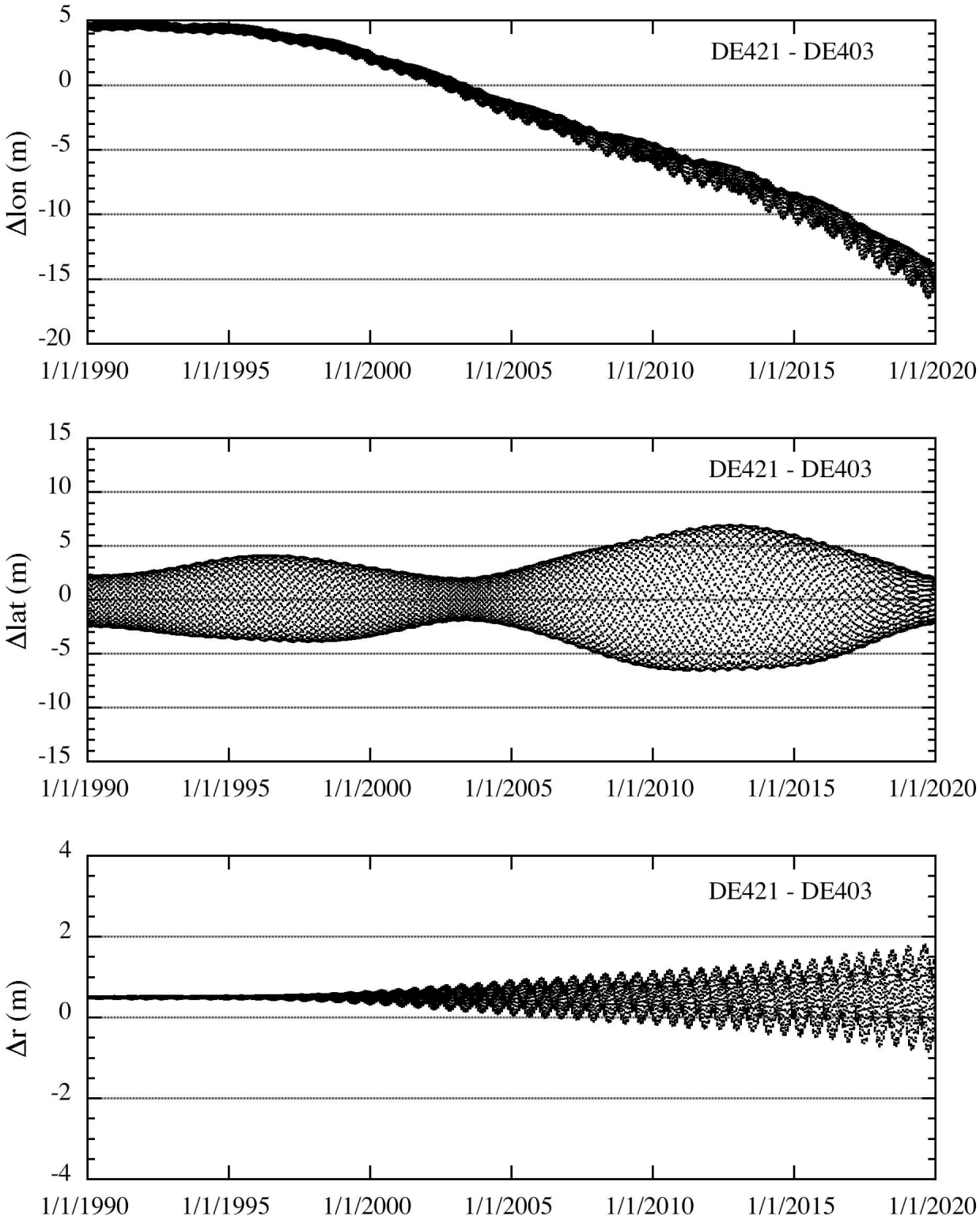

Figure 2. Moon differences for ecliptic longitude and latitude, and radius for DE421 – DE403.

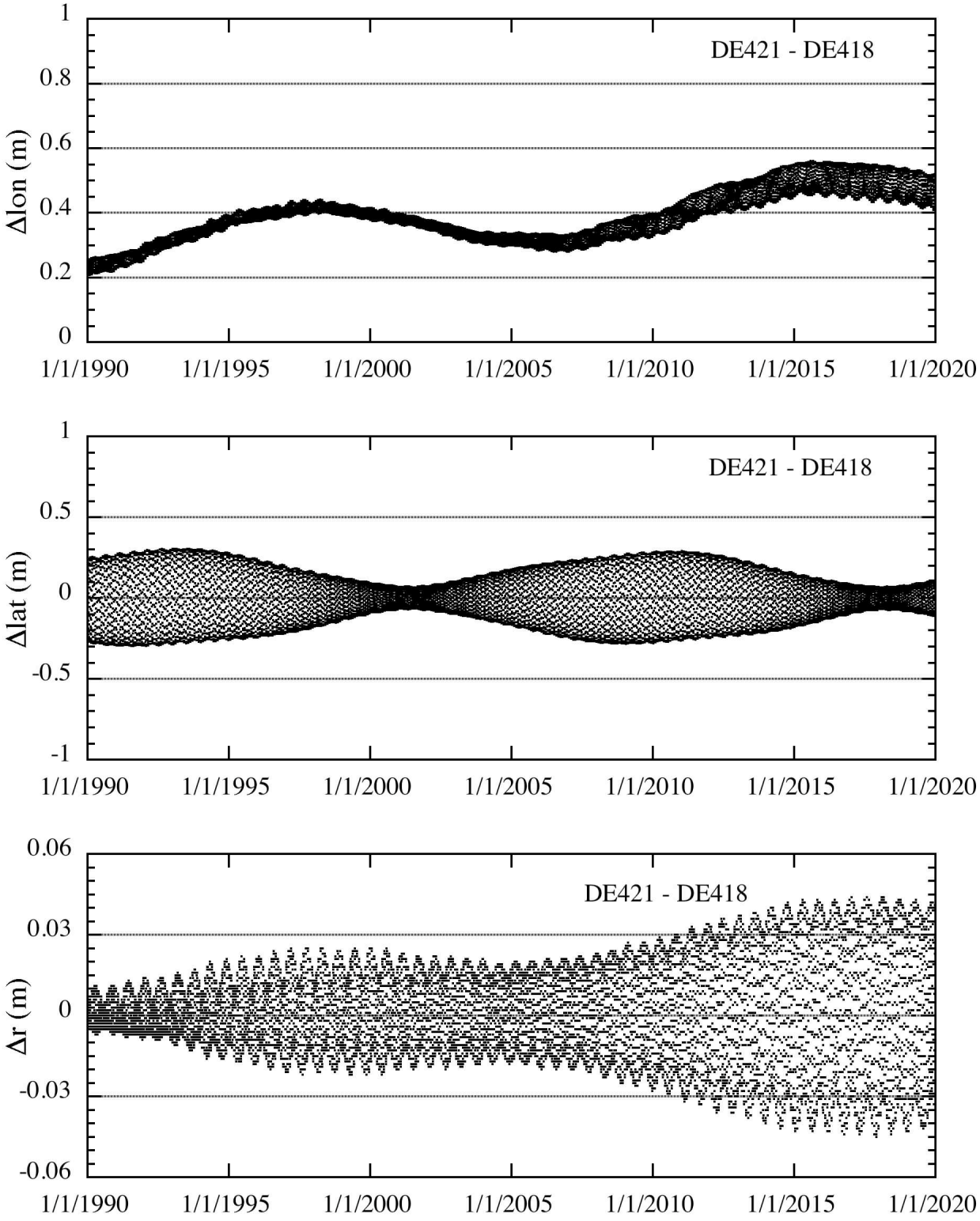

Figure 3. Moon differences for ecliptic longitude and latitude, and radius for DE421 – DE418.

Construction of the Ephemeris

The DE421 planets have been discussed by Folkner et al. (2008). Here we address the lunar ephemeris and rotation. The initial conditions for the lunar ephemeris and three dimensional lunar orientation (Euler angles and spin rates), lunar laser retroreflector array positions and other lunar parameters were fit to Lunar Laser Ranging (LLR) data. A total of 16,601 ranges extend from March 16, 1970 to December 27, 2007. Modern range accuracies are more than an order-of-magnitude more accurate than the early data. Ranges were processed from McDonald Observatory, Texas, Observatoire de la Côte d'Azur, France, Haleakala Observatory, Hawaii, and Apache Point Observatory, New Mexico. A few ranges from Matera, Italy were also processed. Ranges to four retroreflector arrays on the Moon were used. They are located at the Apollo 11, 14, 15 and Lunokhod 2 sites. A majority of the ranges are to the largest array at the Apollo 15 site (77.9%), while Lunokhod 2 gets the fewest number of ranges (2.7%). Apollo 11 and 14 make up 9.8% and 9.6% of the total data set, respectively. Ranges to multiple arrays are important for determining the physical librations and lunar geophysical parameters.

The construction of a new ephemeris involves a series of choices and sometimes compromises. The models for the computation of both the acceleration of the Moon in its orbit and the torques about its center of mass for the numerical integration, and the computation of range for the range data fits, depend on geophysical processes at the Earth and Moon. Some of the geophysical parameters are input and held constant while others are fit to the lunar ranges. Linear constraints between parameters can be applied. Many more lunar parameters were adjusted during the DE421 fit than was the case for DE418 increasing confidence in the final product.

For the Earth's gravity field, J_3 and J_4 were taken from the GGM02C gravity field and the equatorial Earth radius used with gravity was set to 6378.1363 km. The J_2 coefficient was based on the GGM02C "tide free" value, but the J_2 value was adjusted for a different Love number k_{20} used here. The constant part of the zonal ocean tide is part of the tidal acceleration computation here, while that contribution is included in the GGM02C J_2 value, so it is necessary to account for the difference. The tidal gravity model here uses three Love numbers k_{20}, k_{21}, and k_{22} with three tidal time delays for the long period (zonal), diurnal, and semidiurnal tides, respectively. The three Love numbers and the zonal (long period) time delay were combined from separate Earth and ocean tides. Tidal response changes with frequency and values were chosen to approximately match the Mf, O1, and M2 tides, which are the most important tides in each of the three frequency bands for the tidal secular acceleration of the Moon. The Earth tides came from the IERS Conventions (McCarthy and Petit, 2003) and the ocean tides were based on the FES2004 result (Lyard et al., 2006; reformatted by Richard Ray on a web site, 2007). The zonal time delay (Δt_{20}) was based on the Mf ocean tide, but the diurnal (Δt_{21}) and semidiurnal (Δt_{22}) time delays were solution parameters. Combined Earth tide parameters are summarized in Table 1. “Type” indicates whether a parameter was fixed or free to change during the solution, or derived from other parameters after the solution. Tidal secular acceleration in orbital longitude and semimajor axis rate were derived from the tide values using a theory after the solution was complete. The computation of the range depends on the coordinates of the ranging stations which are fit. Station motion was fit when the station’s data span was years. Two rotation angles at J2000 (X rotation about equinox direction and Y about axis at 90˚ right ascension and 0 declination) are fit to orient the Earth’s equator in space with respect to its orbit. The alignment

of the inner four planets with the international celestial reference frame (ICRF) is established mainly through planetary VLBI data to Mars and Venus. The precession and obliquity rates with respect to space and also several nutation coefficients were fit. The X and Y rotation values have some dependence on the secular and long-period variations. The diurnal and semidiurnal UT1 terms were based on the IERS conventions. GM of the Earth+Moon was fixed during solutions, so the value of the Sun/(Earth+Moon) mass ratio and the derived GM_{earth}, using TDB seconds, are not new results.

Table 1. Geophysical and orientation parameters for Earth.

Parameter	Type	Unit	Value
Sun/(Earth+Moon)	fixed	1	328900.55915
GM_{earth}	derived	km^3/sec^2	398600.4362
equatorial radius	fixed	km	6378.1363
k_{20}	fixed	1	0.335
k_{21}	fixed	1	0.320
k_{22}	fixed	1	0.320
Δt_{20}	fixed	day	0.0640
Δt_{21}	fit	day	0.01114245
Δt_{22}	fit	day	0.00657429
zonal dn/dt	derived	$"/cent^2$	0.12
diurnal dn/dt	derived	$"/cent^2$	-3.31
semidiurnal dn/dt	derived	$"/cent^2$	-22.88
zonal da/dt	derived	mm/yr	-0.18
diurnal da/dt	derived	mm/yr	4.89
semidiurnal da/dt	derived	mm/yr	33.75
X axis rotation	fit	mas	5.8
Y axis rotation	fit	mas	-16.9
obliquity rate	fit	mas/yr	-0.26
luni-solar precession	fit	"/yr	50.38490

Table 2 gives the lunar geophysical parameters. In Tables 1 and 2 extended numbers of digits are given for internal consistency; they do not imply accuracy. Some of the lunar gravity field coefficients were fixed to LP150Q values (Konopliv, website) and some were fit, as described in the next section. The radius used with the gravity field was 1738 km, a reasonable value for the equatorial radius, though the mean radius is smaller (Smith et al., 1997). The mass of the Moon depends on the Earth/Moon mass ratio and the GM of the Earth-Moon system. The mass ratio was fit to planetary data. The lunar mantle orientation (physical libration) initial conditions and retroreflector coordinates for Apollo 11, 14, 15 and Lunokhod 2 were solution parameters. These results are given in later sections. Lunar Love numbers h_2 and k_2 were fit, but the ratio was constrained to a model value of 1.75 during the fit. Love number l_2 was fixed to a model value. Dissipation parameters are fit for lunar tides (time delay Δt_m) and fluid-core/solid-mantle interface (CMB) interaction (K_v); see Williams et al. (2001) for definitions. Oblateness of the CMB and initial values for the fluid core orientation were fit. The moment of inertia of the fluid core was set to $7x10^{-4}$ of the total moment, consistent with recent solutions (Williams et al., 2008). The static J_2 coefficient was based on the LP150Q value by applying a constraint which

adjusts for the difference in the constant J_2 tide contribution from the LP150Q k_2 value and the solution value here. The constraint, based on Williams et al. (2001), is

$$J_2 + 3.6987 \times 10^{-6}\, k_2 = 2.033532597 \times 10^{-4} \quad . \qquad (1)$$

C_{22} is calculated from J_2 and the two lunar moment of inertia differences (C-A)/B and (B-A)/C. All four of these values do not include the tidal contributions.

Table 2. Moon geophysical parameters.

Parameter	type	Unit	Value
mass ratio Earth/Moon	fit	1	81.30056907
GM_{moon}	derived	km^3/sec^2	4902.80008
equatorial radius	fixed	km	1738.0
(C-A)/B	fit	1	631.0022×10^{-6}
(B-A)/C	fit	1	227.7305×10^{-6}
J_2	constrained	1	203.27326×10^{-6}
C_{22}	derived	1	22.38977×10^{-6}
k_2	constrained fit	1	0.02163
h_2	constrained fit	1	0.03786
l_2	fixed to model	1	0.01050
Δt_m	fit	day	0.10786
K_v	fit	1/day	1.49376×10^{-8}
tidal dn/dt	derived	"/cent^2	0.20
CMB dn/dt	derived	"/cent^2	0.02
tidal da/dt	derived	mm/yr	-0.30
CMB da/dt	derived	mm/yr	-0.02
core moment/total moment	fixed	1	7×10^{-4}
CMB flattening	fit	1	3.7977×10^{-4}

When the dissipation effects from Earth and Moon are added together, the resulting acceleration in longitude is -25.85 "/cent^2 and the semimajor axis rate is 38.14 mm/yr. These derived values depend on a theory which is not accurate to the number of digits given. The conversion for Earth tides is thought to be accurate to ~1/2% of the total, but that is a rough estimate. Differences between distinct ephemerides are useful, e.g. the computed DE421–DE418 tidal acceleration difference is only 0.01 "/cent^2 and is not evident in Figure 3 while the DE421–DE403 difference of -0.21 "/cent^2 is prominent in Figure 2 as the 4 cm/yr^2 acceleration. Dissipation effects also cause an eccentricity rate, but there is an anomalous rate as well (Williams et al., 2001). Because we do not know the source of this anomalous rate, we cannot include it in the numerical integration model. Consequently, an anomalous eccentricity rate is not solved for here and that is a compromise. Compared to solutions with an independent rate (Williams et al., 2008), the solution here responds by decreasing the dissipation in lunar tides and increasing the dissipation from the CMB interaction and this distorted fit has a slightly larger rms postfit residual. Another compromise is the dependence of the Moon's tidal damping on frequency. The integration model uses a time delay model, corresponding to a tidal Q proportional to 1/frequency, but fits with parameters sensitive to the frequency dependence support only a weak dependence on frequency

(Williams et al., 2001; Williams et al., 2008). The different tidal frequency dependences cause physical libration effects at the few milliseconds of arc level which are not present in the integration; these are detectable with the LLR fits but are not troublesome to most users.

Lunar Surface Coordinate Frames — Principal Axes and Mean Earth/Mean Rotation Axes

The solutions for lunar orientation Euler angles and lunar laser retroreflector array coordinates use the principal axes of the lunar moment of inertia matrix for the X, Y and Z directions. These are principal axes before tidal distortions are applied. It is natural to write and integrate the equations of motion for the lunar Euler angles using the principal axes. The center of mass is used for the origin of Moon-fixed frames.

The other frame of interest uses the mean direction toward the Earth for the X axis and the mean rotation direction for the Z axis. Y completes the right-handed triad. In Lunar Laser Ranging (LLR) papers we have called this the mean Earth/mean rotation axis frame or more tersely the mean Earth/rotation axis frame. In papers by Mert Davies and the IAU/IAG working group on coordinates and rotations (Seidelmann et al., 2007, and earlier papers in this sequence) the designation mean Earth/polar axis frame has been used but this is only a name change and these frames are the same. An ellipsoidal Moon with only a second-degree figure (gravity) would have the mean axis and principal axis frames coincident. Third- and higher-degree representations of the gravity field cause a constant rotation between the two frames (Williams et al, 2006). There is also a small constant rotation due to dissipation effects in the Moon.

A constant three-angle rotation relates the two frames, but our knowledge of the three constant angles depends on the gravity field coefficients and it requires a theory relating them. Since gravity field coefficients can change for different ephemerides, the rotation angles must be compatible with the ephemeris. The gravity harmonic coefficients have improved over the years (Konopliv et al., 1998, 2001). Currently, the LP150Q gravity field (Konopliv, website) is recommended for spacecraft orbit calculations. For DE421, the three third-degree coefficients C_{31}, S_{31} and S_{33} and all of the fourth-degree coefficients match the LP150Q values. In addition, the J_2 value is based on LP150Q after accounting for a difference in Love number k_2 using eq. (1). The four remaining third-degree coefficients, the moment of inertia differences which adjust the relation between C_{22} and J_2, and k_2 were fit during the LLR data analysis. Prior to the application of tidal distortions, C_{21}, S_{21} and S_{22} are zero consistent with principal axis coordinates.

The fits to lunar rotation and orbit are done simultaneously and the numerical integration for orbit and Euler angle evolution is simultaneous. Thus, the lunar Euler angles (physical librations) and orbit on the DE file are compatible and the Euler angles use the principal axis frame. Note also that the LP150Q gravity field (Konopliv, website) uses the principal axis frame, albeit the frame for DE403 with an orientation 4" different from DE421. Use of the JPL DE421 ephemeris file with the LP150Q gravity field is recommended for high accuracy navigation purposes.

There are no equations of motions for Euler angles referenced to mean Earth/mean rotation axes. The numerically integrated Euler angles rotating from space to principal axes that are provided with DE files are inherently more accurate than knowledge of the mean axes. For a given gravity

field, the constant three-angle rotation from principal axes to mean axes is less accurately known than the integrated Euler angles. The constant rotation is typically computed after the fit and integration. If one wishes the orientation of the lunar mean Earth/mean rotation axes, we recommend first extracting the principal axis angles from the file and then rotating by three constant angles given below.

Note that the semianalytical series expressions for angle W along with pole right ascension and declination, given in the IAU/IAG working group documents (Seidelmann et al, 2007, and earlier), are approximations of much lower accuracy than the numerical integrations. By comparing with integrated values, Konopliv et al. (2001) showed that the series expressions for orientation lead to position errors which can exceed 100 m. One of us (JGW) derived the series expressions and that uncertainty is consistent with the level of truncation of the series.

Moon-Centered Coordinates

Rotations between the two lunar coordinate frames were first developed for the Lunar Laser Ranging (LLR) coordinates of retroreflector arrays. The fits to the LLR data use the integrated lunar orbit and the physical libration Euler angles, so the derived retroreflector array coordinates are in the principal axis frame. Techniques have been developed for determining the constant rotation between principal axis coordinates and mean Earth/mean rotation axis coordinates.

The constant rotation between principal axis coordinates and mean Earth/mean rotation axis coordinates depends on the lunar gravity field coefficients and the calculation ultimately rests on a theory. Originally these theories were by Eckhardt, most recently (1981), and the relevant terms are the constant parts of p_1, p_2, and τ . The first two of these are Moon-fixed x and y coordinates of the unit vector normal to the ecliptic plane and the τ refers to the longitude rotation. The constant parts of p_1, p_2, and τ depend mainly on the gravity field and slightly on dissipation effects; knowledge of the gravity field was poor in earlier times and consequently Eckhardt's constant part of the τ angle is a factor of about three larger than the actual value of the angle! Eckhardt provided partial derivatives with respect to the third-degree gravity coefficients, but since there are nonlinearities in the differential corrections the accuracy is limited at some level. In rotating the Moon-centered coordinates of LLR retroreflector arrays from principal axis to mean Earth/mean rotation axis coordinates, LLR first used Eckhardt's constant parts of p_1, p_2, and τ , but later opted for consistency by deriving empirically the rotations between sets of LLR coordinates determined with different integrated ephemerides. Even with the latter procedure, Eckhardt's theory had been used to rotate the earlier set of coordinates which later empirical rotations depended on.

The last LLR array coordinates which used Eckhardt's theory for the rotation were in Williams, Newhall and Dickey (1987). Subsequent LLR coordinates during the past two decades were aligned with those mean Earth/mean rotation axis coordinates: 1) An internal memo (Williams, Newhall and Standish, 1993) gave a set for DE245 prepared at the time of the Clementine mission. 2) Williams, Newhall and Dickey (1996) published a set compatible with the gravity coefficients in Dickey et al. (1994). The 1996 rotations were also given by in a paper by Davies and Colvin (2000), but the coordinates there are slightly different from our 1996 paper. 3) LLR

coordinates using DE403 and the three associated rotations have been distributed by email. These coordinates were used and published while the associated angles for the DE403-related rotations are given in Konopliv et al. (2001) and Seidelmann et al. (2007).

In the DE418 lunar memo (Williams and Folkner, 2007) and in this memo the procedure is changed again. The LLR principal axis coordinates determined during the solution leading to DE421 are given in Table 3. For the rotation to the mean Earth/mean rotation axis frame, the rotation in longitude, which is very sensitive to the gravity field coefficients, was computed from a new theory in order to overcome the less accurate gravity field that Eckhardt (1981) used. The unpublished new theory (from JGW) balances the C_{22} torque from the displaced X and Y axes against the torques from the third- and fourth-degree coefficients. A smaller contribution from tide and core dissipation (Williams et al, 2001) is also added. For the DE418 coordinates, the pole direction from a fit of periodic terms to the DE403 Euler angle orientations by Newhall and Williams (1997) was used with corrections for the difference between DE403 and DE418. Here, the pole direction has used a fit to the DE418 Euler angles by Rambaux (private communication, 2008) converted to p_1 and p_2 and modified for the slight difference between the DE418 and DE421 rotations.

If M is a vector of Cartesian coordinates in the mean Earth/mean rotation (MER) axis frame and P is a coordinate vector in the principal axis (PA) frame, then the derived rotation follows the form

$$M = R_x(-p_2)\, R_y(p_1)\, R_z(-\tau)\, P \qquad (2)$$

where p_1 and p_2 and τ are the constant parts of those parameters. Though p_1 and p_2 are coordinates, they are small and are expressed as angles. The three rotations are small and eq. (2) is only first order in the rotations. A more exact expression might differ by a few milliseconds of arc, a few centimeters in position. For DE421 the rotation between frames is

$$M = R_x(-0.30")\, R_y(-78.56")\, R_z(-67.92")\, P \qquad (3)$$

where the angles are in seconds of arc and the rotations are around the body X, Y and Z axes. The inverse rotation is

$$P = R_z(67.92")\, R_y(78.56")\, R_x(0.30")\, M \qquad (4)$$

Note that rotation of coordinates of eqs. (2) - (4) above and the corresponding rotation of the frames have the opposite sense. Rotation of the LLR principal axis array coordinates of Table 3 to the mean Earth/mean rotation axis frame gives the LLR array coordinates in Table 4.

Because of the changed procedure for calculating the constant rotations, the mean axis coordinates of Table 4 are rotated when compared with those previously distributed for the Euler angles of DE403 and earlier ephemerides. Compared to our DE403 MER axis orientation, the differences (ignoring signs) are 0.53" in longitude (rotation about z axis), 0.25" about the y axis and 0.18" about the x axis. At the lunar surface 1" corresponds to 8.4 m, so the displacement from the DE403 MER axis frame is 5 meters. The DE418 and DE421 MER axis frames are

close. In the future it should be possible to improve upon the three angles for the DE421 rotation between frames in eqs. (2) and (3) further, but the values here should be close enough for meter level accuracy. A separate question is how much the rotation between frames will change for future ephemerides. Gravity field uncertainties for S_{31} and S_{33} are most important for the longitude rotation uncertainty. For the LP150Q coefficients that uncertainty is about 1.0" and future changes in the principal axis direction due to gravity field changes can be of that order. Comparing mean axis coordinates from DE421 and DE403, there is also a shift of 0.7 m along the X axis due partly to changed orbital semimajor axis and GM(Earth+Moon) and partly due to different tidal Love numbers.

Table 3. Lunar laser retroreflector array coordinates using principal axis frame.

Array	X	Y	Z	R	E Longitude	Latitude
	meters	meters	meters	meters	degrees	degrees
Apollo 11	1591967.522	690698.106	21003.309	1735472.732	23.4543075	0.6934309
Apollo 14	1652689.359	-520999.194	-109731.018	1736336.135	-17.4971065	-3.6233288
Apollo 15	1554678.949	98094.117	765004.907	1735477.340	3.6103520	26.1551743
Lunokhod 2	1339364.624	801870.788	756358.470	1734639.009	30.9087426	25.8509928

Table 4. Lunar laser retroreflector array coordinates using mean Earth/mean rotation axis frame.

Array	X	Y	Z	R	E Longitude	Latitude
	meters	meters	meters	meters	degrees	degrees
Apollo 11	1591747.845	691222.345	20397.830	1735472.732	23.4730729	0.6734398
Apollo 14	1652818.934	-520454.721	-110361.346	1736336.135	-17.4786483	-3.6441703
Apollo 15	1554937.875	98605.140	764412.735	1735477.340	3.6285073	26.1333959
Lunokhod 2	1339388.500	802310.872	755849.325	1734639.009	30.9221489	25.8323070

The LLR range model includes solid-body tides on the Moon. That calculation includes a constant displacement in addition to time variations. The constant part of tidal displacements, different for each retroreflector array, are not included in Tables 3 and 4 but they are given in Table 5. These can be added to the Table 3 and 4 locations if precise LLR positions are to be used without a tide model. The lunar displacement Love numbers used during the fit were h_2 = 0.03786 and l_2 = 0.01050, giving few decimeter constant tidal displacements as shown.

Table 5. Constant part of tide displacements.

Array	ΔR	ΔEast	ΔNorth
	meters	meters	meters
Apollo 11	0.373	- 0.148	-0.004
Apollo 14	0.420	0.116	0.023
Apollo 15	0.344	-0.023	-0.160
Lunokhod 2	0.192	-0.161	-0.117

Files

The DE421 ephemeris may be downloaded in an ascii version from

ftp://ssd.jpl.nasa.gov/pub/eph/planets/ascii/de421 .

The complete set of input parameters for the solar system integration, more extensive than Tables 1 and 2, is part of the file. The SPICE kernal version of DE421 is available at

ftp://ssd.jpl.nasa.gov/pub/eph/planets/bsp .

Summary

The DE421 lunar position should be an improvement over DE403 at the present time and for years into the future. DE421 and DE418 are much more similar to one another than to the much older DE403. For high accuracy purposes such as lunar navigation, we recommend use of the DE421 JPL ephemeris file with the LP150Q gravity field. Tables 1 and 2 give geophysical parameters used for the Earth and Moon, respectively. Rotation of Moon-centered coordinates between the mean Earth/mean rotation axis frame and the principal axis frame can be achieved with eqs. (3) and (4). Coordinates of the lunar laser retroreflector arrays are given in Tables 3 and 4.

Acknowledgments. We thank Nicolas Rambaux for the physical libration rotation information. The research described in this paper was carried out at the Jet Propulsion Laboratory of the California Institute of Technology, under a contract with the National Aeronautics and Space Administration.

References

Davies, M. E., and T. R. Colvin, Lunar coordinates in the regions of the Apollo landers, *J. Geophys. Res., 105,* 20277-20280, 2000.

Dickey, J. O., P. L. Bender, J. E. Faller, X X Newhall, R. L. Ricklefs, J. G. Ries, P. J. Shelus, C. Veillet, A. L. Whipple, J. R. Wiant, J. G. Williams, and C. F. Yoder, Lunar Laser Ranging: a Continuing Legacy of the Apollo Program, *Science*, *265*, 482-490, 1994.

Eckhardt, D. H., Theory of the libration of the Moon, *Moon and Planets, 25*, 3-49, 1981.

Folkner, W. F., E. M. Standish, J. G. Williams, D. H. Boggs, Planetary and lunar ephemeris DE418, IOM 343R-07-005, August 2, 2007.

Folkner, W. F., J. G. Williams, D. H. Boggs, Planetary ephemeris DE421 for Phoenix navigation, IOM 343R-08-002, February 13, 2008.

Konopliv, A. S., A. B. Binder, L. L. Hood, A. B. Kucinskas, W. L. Sjogren, and J. G. Williams, Improved gravity field of the Moon from Lunar Prospector, *Science, 281*, 1476-1480, 1998.

Konopliv, A. S., S. W. Asmar, E. Carranza, W. L. Sjogren, and D. N. Yuan, Recent gravity models as a result of the lunar prospector mission, *Icarus, 150*, 1-18, 2001.

Konopliv, A. S., the LP150Q lunar gravity field is available on the PDS website http://pds-geosciences.wustl.edu/geo/lp-l-rss-5-gravity-v1/lp_1001/sha/jgl150q1.lbl

Lyard, F., F. Lefevre, T. Letellier, and O. Francis, Modelling the global ocean tides: insights from FES2004, *Ocean Dynamics, 56*, 394-415, 2006.

McCarthy, D. D., G. Petit (eds.), IERS Conventions (2003), IERS Technical Note No. 32, 2003.

Newhall, X X, and J. G. Williams, Estimation of the Lunar Physical Librations, *Celestial Mech. and Dyn. Astron., 66*, 21-30, 1997.

Ray, R., http://bowie.gsfc.nasa.gov/ggfc/tides/harm_fes04.html, 2007.

Seidelmann, P. K., B. A. Archinal, M. F. A'Hearn, A. Conrad, G. J. Consolmagno, D. Hestroffer, J. L. Hilton, G. A. Krasinsky, G. Neumann, J. Oberst, P. Stooke, E. F. Tedesco, D. J. Tholen, P. C. Thomas, and I. P. Williams, Report of the IAU/IAG working group on cartographic coordinates and rotational elements: 2006, *Celestial Mechanics and Dynamical Astronomy, 98 (3)*, 155-180, 2007.

Smith, D. E., M. T. Zuber, G. A. Neumann, and F. G. Lemoine, Topography of the Moon from the Clementine lidar, *J. Geophys. Res., 102,* 1591-1611, 1997.

Williams, J. G., Newhall, X X, and Dickey, J. O., Lunar Gravitational Harmonics and Reflector Coordinates, in the proceedings Figure and Dynamics of the Earth, Moon and Planets, astronomical institute of the Czechoslovak academy of sciences research institute of geodesy, topography and cartography, Prague, Czechoslovakia, ed. P. Holota, 643-648, 1987.

Williams, J. G, X X Newhall, E. M. Standish, DE 245 Earth and Moon, JPL Memo, December 17, 1993.

Williams, J. G., X X Newhall, and J. O. Dickey, Lunar Moments, Tides, Orientation, and Coordinate Frames, paper for MORO meeting, June 8-10, 1995 in Pisa, Italy, *Planetary and Space Science, 44*, 1077-1080, 1996.

Williams, J. G., D. H. Boggs, C. F. Yoder, J. T. Ratcliff, and J. O. Dickey, Lunar rotational dissipation in solid body and molten core, *J. Geophys. Res., 106*, 27933-27968, 2001.

Williams, J. G., S. G. Turyshev, D. H. Boggs, and J. T. Ratcliff, Lunar Laser Ranging Science: Gravitational Physics and Lunar Interior and Geodesy, 35th COSPAR Scientific Assembly, July 18-24, 2004, Paris, France, in *Advances in Space Research, vol. 37, Issue 1*, The Moon and Near-Earth Objects, 67-71, doi: 10.1016/j.asr.2005.05.13, 2006. [arXiv:gr-qc/0412049]

Williams, J. G., and W. F. Folkner, DE418 Moon and Lunar Coordinates, IOM 335-JGW,WMF-20071024-002, October 24, 2007.

Williams, J. G., D. H. Boggs, and J. T. Ratcliff, Lunar Tides, Fluid Core and Core/Mantle Boundary, abstract #1484 of the *Lunar and Planetary Science Conference XXXIX,* March 10-14, 2008.